This manuscript has been published online in: Journal of Dentistry, July 2019

https://doi.org/10.1016/j.jdent.2019.06.009

Title: A zinc oxide-modified hydroxyapatite-based cement favored sealing ability in endodontically treated teeth

Short title: Zinc favored sealing of root dentin

Authors: Manuel Toledano[1a], Esther Muñoz-Soto[1b], Fátima S. Aguilera[1a], Estrella Osorio[1a], M. Paloma González-Rodríguez[1a], Mayra C. Pérez-Álvarez[2a], Manuel Toledano-Osorio[1c]*, Raquel Osorio[1a]

Institution: [1]University of Granada, Faculty of Dentistry, Dental Materials Section.
Colegio Máximo de Cartuja s/n
18071 – Granada - Spain.
[2]University of La Havana, Biomaterials Department,
San Lázaro y L. Municipio Plaza de la Revolución
La Havana- Cuba.

Academic positions: [a] Professor
[b] Associate Professor
[c] Student

***Corresponding author:**
Manuel Toledano-Osorio.
University of Granada, Faculty of Dentistry
Colegio Máximo de Cartuja s/n
18071 – Granada - Spain.
Tel.: +34-958243789
Fax: +34-958240809
Email: mtoledano@correo.ugr.es

Keywords: hydroxyapatite, mechanics, remineralisation, root dentine, zinc

Title: A zinc oxide-modified hydroxyapatite-based cement favored sealing ability in endodontically treated teeth.

ABSTRACT

Objectives: To evaluate the effectiveness of different endodontic canal sealers for dentin permeability reduction and to determine the viscoelastic performance of root dentin after their application.

Methods: Cervical, medial and apical root dentin surfaces were treated with two experimental hydroxyapatite-based cements, containing sodium hydroxide (calcypatite) or zinc oxide (oxipatite); an epoxy resin- based canal sealer, AH Plus; and gutta-percha. Root dentin was evaluated for fluid filtration. Field emission scanning electron microscopy, energy dispersive analysis, AFM, Young's modulus and Nano-DMA analysis were also performed, at the inner and outer zones of dentin.

Results: Dentin treated with oxipatite showed the lowest microleakage among groups with hermetically sealed tubules and zinc-based salt formations. Samples treated with oxipatite showed the highest *Ei* at the cervical dentin third among groups, at 6 m of storage. Oxipatite promoted the highest complex modulus and tan delta values at the inner zone of both cervical and medial root dentin. Calcypatite favored the lowest tan delta outcomes at the inner zone of apical dentin at 6 m.

Conclusions: Specimens treated with oxipatite showed the highest sealing ability, based on the highest Young's modulus and dentin mineralization, achieved by closing dentinal tubules, voids and pores that reinforced the inner zone of root dentin. The homogeneity of viscoelastic properties among the different root dentin thirds favored the energy dissipation without creating zones of stress concentration and micro-cracking which would have challenge micropermeability. Thereby, among the tested materials oxipatite is proposed as canal filling material and sealer in endodontics.

Clinical Significance: Oxipatite could be considered a good candidate for root canal filling material and sealer due to its improved long-term sealing ability and to the advanced remineralization, and so to the enhanced energy dissipation achieved at the inner zone of the radicular dentin.

Keywords hydroxyapatite, mechanics, remineralisation, root dentine, zinc.

1. Introduction

Endodontically treated teeth are more likely to fracture than vital teeth because of the loss of tooth structure due to caries, access cavity preparation, and instrumentation of root canal. Both elastic deformation and crack propagation determine the mechanical performance of dentin. Microcracks are found very often in radicular dentin, being pre-existing microcracks or of iatrogenic nature [1]. The availability of endodontic materials with suitable bioactivity aimed to obliterate microcraks, voids, pores and capillary channels is a requirement for the success of the current root canal therapy. In order to ensure this permanent sealing ability, the material must show no disintegration and stability when in contact with physiological fluids [2,3]. A contemporary endodontic treatment technique requires a core material such as gutta-percha and a canal sealer with a dual resin or specific endodontic cement.

Root canal sealers can be inert or able to induce mineral deposition, directly related to their chemical constitution [4]. The contribution of glass-ionomer cements to root canal seal is controversial as they are susceptible to water sorption and leaching [5]. The Portland-based Mineral Trioxide Aggregate cement (MTA) [6] has been used in endodontic field. However, Portland-based materials exhibited long setting time [7], time solubility [8], reduced handling [9], potential discoloration of teeth [10] and a high cost [9]. Moreover, it has been recently reported that root-end fillings performed with MTA may be affected by microleakage after 6 months of water storage [11]. Root canal sealers based on epoxy resins such as AH-Plus have been recognized as "gold standard" among endodontic materials to obtain adhesion to root dentin surface but doubts about toxicity and dentin regeneration question their use [12].

Intracanal medicaments containing calcium hydroxide [$Ca(OH)_2$] are employed in regenerative endodontics [13], but they seem to favor root fracture. Calcium hydroxide powder in association with hydroxyapatite (HAp), as vehicle, has been proposed for repair and regeneration of hard tissues [14]. Nevertheless, HAp possesses low mechanical strength and fracture toughness, which is an obstacle for its application in load-bearing areas [14]. Zn-substituted HAp has been shown to possess enhanced bioactivity. This effect makes zinc attractive for use as therapeutic agent in the fields of hard tissue regeneration [15].

To investigate the changes in the mechanical properties of root dentin associated with cervical, middle or apical regions after applying different endodontic sealers, atomic force microscopy (AFM)-based nano-indentation and surface morphology were determined. Scanning electron microscope in combination with energy dispersive X-rays analyzer (FESEM/EDX) were also done. The aim of this study was to evaluate the flow rate, thorough endodontically treated roots as an index of sealing ability, to assess the Young's modulus as an index of mineralization, and viscoelastic behavior of radicular dentin interfaces treated with four root canal filling materials used as sealers in association with gutta-percha. The tested null hypothesis was that the endodontic sealer selection does not influence dentin micropermeability, neither Young's modulus and viscoelasticity, evaluated at the interfaces, over time.

2. Materials and methods

2.1. Specimen preparation and cement application

Sixty four human mandibular premolars with single roots and vital pulp, extracted for orthodontic or periodontal reasons, without caries lesions were obtained with informed consent from donors (18–25 yr of age), under a protocol approved by the Institution Review Board (#139/CEIH/2016). The teeth were randomly selected and stored at 4ºC in 0.5% chloramine T bacteriostatic/bactericidal solution for up to 1

month. This storage medium was replaced weekly. All teeth were integral and examined using a stereomicroscope (Olympus SZ-CTV, Olympus, Tokyo, Japan) to ascertain the absence of any root fracture or craze lines. The teeth were decoronated using a low-speed diamond saw (Accutom-50 Struers, Copenhagen, Denmark), and the root length was standardized to approximately 12 mm. and radiographed at 2 angulations to confirm the presence of a single canals. The rest of the root canal treatment was as in Mestres et al [3].

Two experimental hydroxyapatite-based cements were used: *i*) Calcypatite composed by modified hydroxyapatite particles and a calcium hydroxide-based paste and *ii*) Oxipatite which is a combination of the hydroxyapatite particles and zinc oxide (ZnO). (*iii*) AH PLUS cement (Dentsply, DeTrey, Konstanz, Germany) and finally *(iv)* guttapercha (GuttaCore) (Dentsply Maillefer, Ballaigues, Switzerland) was compacted into the radicular canal without any sealer or cement. A detailed description of the chemicals and cements is provided in Table 1. Sixteen teeth were treated with each cement type. Cements were introduced into the root using a lentulo spiral [3,16,17]. The cements, used as filling materials (calcypatite and oxipatite), or as sealer (AH-PLUS), were compacted into the radicular canal with an endodontic plugger. For gutta-percha, one size 30 GuttaCore (GC) cone was placed into the canal to working length, in all groups.

2.2. Sealing ability trough the fluid filtration system

Forty samples were employed for this part of the study. Ten specimens were tested for each cement type. After storing the filled root canals in SBFS for 24 h, teeth were covered with two layers of varnish up to 2 mm from the root apex. The provisional restoration was removed and the coronal part was fixed on a Plexiglass support with cyanoacrylate adhesive (Rocket, Corona, CA, USA); the support was penetrated by an 18-gauge needle, which was introduced 2 mm into the root coronal portion. To measure the microfiltration of the filled roots, the other side of the 18-gauge needle was introduced into an 18-gauge polyethylene tubing (R-3603, Tygon, Paris, France) of the fluid filtration system. The fluid flow of the filled root canals was measured using a liquid flow sensor (ASL 1600, Sensirion, Staefa, Switzerland), which was connected between the source of hydraulic pressure and the root specimen. A constant hydraulic pressure of 6.86 kPa was generated by suspending a syringe filled with 60 mL of deionized water 70 cm above the sensor (Fig 1a). The fluid flow rate of every specimen (out of 10 for each formulation) was measured for 30 s and repeated 10 times in succession, after 5 min of fluid stabilization (total measurements n = 100). The fluid flow through the root canal was measured at different time periods: 24 h, 1 week and 1, 3 and 6 months [18]. The specimens were stored in SBFS and the medium was refreshed every 2 weeks.

2.3. Nanoindentation

Twenty four teeth were employed in this part of the study. Six teeth per cement type were employed. 50% of the specimens were tested at 24 h and the other after 6 m of storage. From each root, three dentin blocks were obtained. The crowns were removed at the cement-enamel junction, using a water-cooled diamond saw (Accutom-50 Struers, Copenhagen, Denmark). The roots were then sectioned bucco-lingually through the centre of the root canal, in order to obtain three sample slabs with a thickness of 1 mm, from cervical, middle and apical areas for evaluation. The surfaces were polished through SiC abrasive papers from 800 up to 4000 grit followed by final polishing steps performed using diamond pastes through 1 μm down to 0.25 μm (Struers LaboPol-4;

Struers GmbH, Hannover, Germany) (Fig 1b). The specimens were treated in ultrasonic bath (Model QS3, Ultrawave Ltd, Cardiff, UK) containing deionized water for 5 min at each polishing step.

a) Young's Modulus and Nano-DMA analysis

A Hysitron Ti-750D TriboIndenter (Hysitron, Inc., Minneapolis, MN) equipped with a commercial nano-DMA package was employed in this study. The nanoindenter was a Berkovich (three sides pyramidal) diamond tip (tip radius ~20 nm). The nanoindenter tip was calibrated against a fused quartz sample using a quasistatic force setpoint of 5 μN to maintain contact between the tip and the sample surface. Based on a calibration-reduced modulus value of 1.1400E+03 N/mm^2 for the fused quartz, the best-fit spherical radius approximation for tip was found to be 150 nm. On each slab, ten indentation were executed in two different mesio-distal positions [20 μm next to radicular cement (outer zone) and 20 μm next to radicular canal (inner zone)] (Fig 1b) along the dentin surface in a straight line. Indentations were performed with a load of 4000 nN and a time function of 10 s. The indenter was progressively (at a constant rate) pressed over the sample up to a peak load of 4000 μN. Specimens were scanned in a hydrated condition. To avoid dehydration a layer of ethylene glycol over the specimen surface was applied, preventing water evaporation during a typical 25-to-30-min scanning period [19]. The rest of the procedures were as in Oliver and Pharr [20] and Toledano et al. [21].

Further dentin disks were subjected to nano-DMA analyses. A dynamic (oscillatory) force of 2 μN was superimposed on the quasistatic signal at a frequency of 200 Hz. Based on a calibration-reduced modulus value of 69.6 GPa for the fused quartz, the best-fit spherical radius approximation for tip was found to be 150 nm, for the selected nano-DMA scanning parameters. Modulus mapping was conducted by imposing a quasistatic force setpoint, Fq=2 μN, to which it was superimposed a sinusoidal force of amplitude FA=0.10 μN and frequency f=100 Hz. The resulting displacement (deformation) at the site of indentation was monitored as a function of time. Data from regions, approximately 20×20 μm in size, were collected using a scanning frequency of 0.2 Hz. Specimens were scanned under a hydrated condition. In order to accomplish for this purpose, samples were stored in PBS after polishing to maintain the hydration. The rest of the procedure was as in Toledano-Osorio et al. [22].

b) Atomic Force Microscopy (AFM)

An atomic force microscope (AFM Nanoscope V, Digital Instruments, Veeco Metrology group, Santa Barbara, CA, USA) was employed in this study for topography mappings. The imaging process was undertaken inside a fluids cell of the AFM in a fully hydrated state, using the tapping mode, with a calibrated vertical-engaged piezo-scanner (Digital Instrument, Santa Barbara, CA, USA). A 10 nm radius silicon nitride tip (Veeco) was attached to the end of an oscillating cantilever that came into intermittent contact with the surface at the lowest point of the oscillation [22].

2.4. Field Emission Scanning Electron Microscopy (FESEM) and energy dispersive (FESEM/EDX) analyses

After nano-DMA and AFM analysis, specimens were fixed in a solution of 2.5% glutaraldehyde in 0.1 mol/L sodium cacodylate buffer for 24 h. Samples were subjected to critical point drying (Leica EM CPD 300, Wien, Austria), sputter-coated with carbon by means of a sputter-coating Nanotech Polaron-SEMPREP2 (Polaron Equipment Ltd., Watford, UK) and observed with a field emission scanning electron microscope

(FESEM Gemini, Carl Zeiss, Oberkochen, Germany). Energy-dispersive analysis was also performed in selected points using an X-ray detector system (EDX Inca 300, Oxford Instruments, Oxford, UK) attached to the FESEM. FESEM and EDX analyses were performed at 24 h and 6 m of SBFS storage.

2.5. Statistical methods

Statistical analysis was performed for dentin permeability and nano-DMA evaluations with ANOVA, Student Newman Keuls multiple comparisons ($P<0.05$) and Student *t* tests ($P<0.01$).

3. Results

The fluid filtration rate ($\mu L\ min^{-1}$) for the four groups at different storage time (24 h-6 months) is shown in Fig. 2. Statistically significant differences ($P<0.05$) were found among sealers. In detail, samples treated with both guttacore and AH Plus did not show any change in microleakage over time ($P<0.05$). Specimens treated with calcypatite did not change their microleakage values over time after 1 week of storage ($P<0.05$), showing a stable seal. Specimens treated with oxipatite did not modify their microleakage values over time, except atter 1 week of storage when it increased ($P<0.05$). Root dentin treated with oxipatite showed the lowest microleakage among groups at 1, 3 and 6 month of storage ($P<0.05$).

The modulus of Young (*Ei)* of dentin surfaces was influenced by the type of canal filler ($P<0.05$), dentin third ($P<0.05$), dentin zone ($P<0.05$) and by the storage time ($P<0.05$). Interactions between factors were also significant ($P<0.05$). Mean and SD of *Ei* at the three different dentin disks (cervical, medial and apical) and zones (inner and outer dentin) are represented in Table 2. Samples treated with oxipatite showed the highest *Ei* at both inner and outer zones of cervical dentin third, at 6 m of storage time (Table 2). Samples treated with oxipatite increased their modulus of Young over time at the inner zone of cervical and apical dentin. At the inner zone of the apical dentin third, specimens treated with both calcypatite and oxipatite cements obtained the highest *Ei* at 6 m of storage, and samples treated with oxipatite increased their values over time. At the outer zone of dentin, samples treated with oxipatite showed the highest *Ei* values among groups, and *Ei* did not change over time. After 6 m of storage, the inner zone of apical dentin treated with oxipatite also attained the highest *Ei* among dentin thirds.

After 6 m of storage, at the inner zone of cervical and medial dentin all samples attained similar storage modulus (*E′*). Dentin treated with calcypatite showed the highest *E′* at the inner apical dentin, and all samples performed similar at the outer zone (Table S1). After 6 m of storage, at the inner zone of cervical dentin samples treated with both AH Plus and GuttaCore attained similar loss modulus (*E″*) that was lower than that of oxipatite and calcypatite. *E″* was similar, among groups, after 6 m time point at the inner or outer medial and apical dentin thirds (Table S1). At the apical dentin third, samples treated with calcypatite attained the highest complex modulus (*E**) values at the inner zone after 6 m of storage (Figs S1a, S2c), and AH plus promoted the lowest values; at the outer zone differences were not encountered. *E** assessed at the inner zone of cervical and medial dentin thirds showed similar values among groups at 6 m of storage, meanwhile specimens treated with oxipatite achieved the highest values, and AH Plus the lowest, at the outer zone of cervical dentin (Figs S1a, S2d). After 6 m of storage, tan delta (δ) at the inner and outer zones of cervical and medial dentin thirds showed the highest values when oxipatite was used (Fig S1b). Inner dentin treated with oxipatite, after 6 m, showed peritubular (double arrows) and intertubular (asterisks) dentin strongly remineralized. Knob-like mineral precipitates (faced arrows) deposited

on the dentin surface. No sign of stress concentration was discovered through the dentin surface due to the highest homogeneity of viscoelastic properties among the different dentin thirds, especially at the tan δ values (Fig. 3a). Multiple rods-like bodies (arrows) linked those crystal precipitates. Special mineral formations, combination of both straight rods (4c·I, c·II) and knob-like precipitates (4c·II), were observed at the interface. At the inner zone of the apical dentin third, samples treated with calcypatite achieved the lowest tan delta (δ) values. Samples treated with calcypatite, after 6 m showed stick-slip images in radial direction of nucleated minerals which resulted observable at the intertubular dentin, as sight of energy dissipation (arrowheads) Extended mineral-depleted areas (faced arrows) are reflected. The crack deflection and branching around the peritubular cuff, may be observed at the dentin wall of an unfilled tubule (single arrows). Strong processes of intertubular and intratubular mineralization, with protruding rounded forms were also observed (faced double arrows) (Fig. 3b). Mineral exhibited multiform clumps of material scattered, uneven, grouped or interconnected as dense network of buttons-like materials, rounding (4d·II, 4e·II) or amorphous (4f·II). Strong mineralization of peritubular dentin was detectable and minerals formed a collar around the narrowest ring of the tubule lumen (arrowheads) (4d·II, 4e·I, 4e·II), and some porosities were detected at the interface (asterisks). At the outer dentin zone both AH Plus and oxipatite showed the lowest values (Fig S1b). When AH Plus was used after 6 m of immersion, firm partial (arrows) or total (asterisks) tubular occlusion was shown. Opened dentinal tubules are observed (double arrows). Some bridge and rod-like new mineral formations were observed surrounding the intratubular crystals (faced arrows). These crystals precipitated beams held the intratubular deposits of mineral to the peritubular dentin. Microcraks (double faced arrows), located at the limits between the peritubular and intertubular dentin, may be shown parallel to the intratubular mineral deposits (Fig. 3c).

Samples treated with calcypatite showed both dentinal tubules totally filled, partially occluded with calcium-phosphate formations, or mineral-free (Figs 3b, 4c). Specimens treated with oxipatite showed, in general, hermetically sealed tubules and zinc-based salt formations (Figs 3a, 4d). With both canal sealers, peritubular dentin appeared strongly mineralized. Gaps were observed at the resin and dentin interface when AH Plus was employed (Figs 3c, 4g).

4. Discussion

Obturating instrumented root canals with oxipatite, a combination of hydroxyapatite particles and zinc oxide, reinforces the inner root zone at any third of radicular dentin. This was achieved by increasing Young's modulus, remineralization, resistance to dynamic deformation and potential for recoil and /or failure and, as a consequence, sealing ability. The direct contact of canal sealer cements with dentin, *i.e* inner zone, may challenge wound healing and affect sealing [18]. Samples treated with oxipatite increased the modulus of Young over time at the inner zone of cervical (~22 GPa) and apical (~26 GPa) dentin (Table 2). The outcomes obtained in the present study may be interpreted as result of a higher mineralization [23], and was linked to mineral precipitation (Ca, P and Zn) within the demineralized organic matrix.

The determined Young's modulus for permanent dentin has been 24.4 GPa [24]. Xu et al. [25] obtained data, ranging from 16.45 to 24.47 GPa consistent with that obtained at cervical, medial and distal regions in the present research (Table 2). The highest *Ei* values (25.99 GPa) were attained at the inner apical dentin when oxipatite was used, at 6 m of storage time. The presence of Zn^{2+} in oxipatite applied on dentin performs as

Ca/P growth inhibitors [26], favoring intrafibrillar mineralization of collagen [27] linked to the raise of *Ei* (Table 2). Thus, root dentin treated with oxipatite showed, in general, the lowest microleakage among groups over time (Fig 2). This improved sealing ability was associated with the formation of hydroxyapatite (Figs 3a, 4d, 4e, 4f) that would obliterate voids, pores and capillary channels [7]. Additionally, an efficient remineralizing effect would require the capacity to absorb mechanical shock waves in order to prevent crack generation and propagation across the dentin surface. The presence of cracks influencing microleakage reinforces the assumption that they can facilitate the penetration of fluids and acids, which demineralize the hydroxyapatite around it, producing not only fracture but also recurrent caries [28].

Considering that both the storage modulus (E') and the loss modulus (E'') are involved in the viscoelastic expression of the complex modulus (E^*) and tan δ, only E^* and tan δ will be discussed. The complex modulus is a measure of the resistance of a material to dynamic deformation [29]. High different modulus (E^*) at the inner zones of cervical dentin were observed close to relatively low elastic modulus inner zones of medial dentin when both calcypatite (Figs 4a, 4b, S2a, S2b) and oxipatite (Figs 4d, 4e) were used (Fig. S1a). As a result, E^* differences between cervical and medial root dentin treated with oxipatite were lower (~2.37 fold) than that obtained when calcypatite was employed (~3.31 fold). Differences were also higher in samples treated with calcypatite than with oxipatite when medial and apical inner dentin zones were respectively compared (~3.38 *vs* 1.34 fold). Root dentin surfaces treated with oxipatite at cervical/middle inner zones (Figs 4d, 4e, 4f, S2d, S2e) showed null ratios of tan δ values (~0.0 fold) in comparison to calcypatite (~0.3 fold) after 6 m of storage (Fig S1b). The lower tan δ, the greater the proportion of energy available in the system for recoil and/or failure [30]. This homogeneous viscoelastic performance was not associated to any sign of energy concentration which hardly appeared at the dentin surface treated with oxipatite (Fig. 3a) [31]. Perhaps, the higher mineralization of dentin with oxipatite, at the expense of zinc-based salts that formed in dentin (Fig 4a) and at the pulp canal sealer surface (Fig. 4b) able to fill the open voids [18], results in an increase of cohesion within the dentin constituents. As a consequence, no signs of stress concentration nor crack deflection were observed contributing to the low microleakage scores and permeability that were reported, explaining the stable sealing ability demonstrated over time by oxipatite (Fig. 2).

Generally, specimens treated with calcypatite did not change their microleakage values over time, and showed lower sealing ability (Fig. 2) than oxipatite (Figs. 3b, 4b, 4h·I). Furthermore, the inner zone of dentin decreased its *Ei* values over time, when calcypatite was used as canal sealer at both cervical and medial dentin disks (Table 2), denoting poor remineralization potential (Figs. 4d, 4e, 4f) after 6 m time. Dentinal tubules appeared partially filled or empty, reflecting scarce presence of intratubular mineralization in comparison to samples treated with oxipatite (Figs. 4a, 4b, 4c). The topography mapping obtained by AFM confirmed the existence of a neat stick-slip image at the peritubular-intertubular dentin edge, in samples treated with calcypatite at 6 m time point (Fig. 3b). These stick-slip images and little rod-like minerals appeared at the dentin surface as bridge-like structures [31] that might be influential in effectively resisting crack propagation leading to fracture [32] by nucleating minerals at micro (Fig S3b) and nano-scales (Fig 3b) cracked zones. These microcraks contribute to the damage of the quality parameters of the dentin [32], though dentin exhibits a rising crack growth resistance with crack extension due to its hierarchical microstructure [33]. The bridge also appeared in the walls of dentinal tubules or even beyond these

structures [34], where an extended layer of new mineral with frictional pullout crossed over a part of the dentin surface (Fig S3a). Those formations were absent in samples treated with oxipatite (Fig. 3a). Nevertheless, this calcified barrier is porous, composed of micro-channels [18], and weakens roots when placed for extended periods [35], favoring microleakage (Fig 2) and low mechanical properties in case of using calcypatite (Table 2).

AH Plus contains Epoxi resins which has been demonstrated to suffer from traces of moisture and the sealing process is negatively affected by the internal dentine wetness which favors local detachment and marginal gaps between the dentin and the canal sealer [18] (Figs. 3c, 4g). Thus, calcypatite application provoked one of the lowest mechanical properties at both 24 h and 6 m in the different dentin thirds, which denotes poor functional or intrafibrillar remineralization [36], slowing down the active dentin remodeling, with decreased maturity and low mechanical properties [23]. This discouraged its indication for endodontic sealer, and oxipatite is preferred. In general, specimens treated with oxipatite reproduced the greater sealing ability, *i.e*, the lowest microleakage among groups (Fig. 2). Thereby, oxipatite could be considered good candidate as root canal filling material and sealer due to its improved long-term sealing ability.

Although the results further establish the importance of including zinc oxide in the chemical formulation of hydroxyapatite based cements for endodontic purposes, there are recognized limitations, *e.g*, differences in microstructure between sound and caries affected root dentin. Endodontic treatment can introduce flaws which can lead to premature failure of the tooth as a result of a catastrophic failure, or more plausible, subcritical crack growth induced by cycling-fatigue loading [37]. Nevertheless, these are to the best of our knowledge the only available results from nano-DMA experiments with morphological characterization from root dentin treated with Zn oxide-modified and calcium hydroxide apatite-based cements. Based on this reasoning, the null hypothesis that was established must be rejected.

5. Conclusions

GuttaCore alone or with AH Plus did not efficiently promote sealing and remineralization of the radicular dentin. Calcypatite produced non-functional mineralization and micropermeability due to porosities and scarce energy dissipation. Specimens treated with oxipatite, a combination of hydroxyapatite particles and zinc oxide, showed the highest sealing ability. The lowest microleakage among groups that attained was based on the highest modulus of elasticity and dentin mineralization that was achieved by closing dentinal tubules, voids, pores and capillary channels. The homogeneity of viscoelastic properties among the different root dentin thirds contributed to the energy dissipation without creating zones of stress concentration and micro-cracking which would have favored micropermeability. Thereby, within the limitation of the present study, oxipatite is proposed as canal filling material and sealer due to, in addition, its improved long-term sealing ability.

Declaration of interest

The authors declare that they have no conflict of interest.

References

[1] T. Brosh, Z. Metzger, R. Pilo, Circumferential root strains generated during lateral compaction with stainless steel vs. nickel-titanium finger spreaders, Eur. J. Oral Sci. 126 (2018) 518–525. doi:10.1111/eos.12569.

[2] G. Bergenholtz, P. Horsted-Bindslev, C. Reit, Textbook of Endodontology, 2nd Edition, Wiley-Blackwell, London, 2009. https://books.google.es/books?id=lpLHCQAAQBAJ.

[3] G. Mestres, F.S. Aguilera, N. Manzanares, S. Sauro, R. Osorio, M. Toledano, M.P. Ginebra, Magnesium phosphate cements for endodontic applications with improved long-term sealing ability, Int Endod J. 47 (2014) 127–139. doi:10.1111/iej.12123.

[4] R. Viapiana, J.M. Guerreiro-Tanomaru, M.A. Hungaro-Duarte, M. Tanomaru-Filho, J. Camilleri, Chemical characterization and bioactivity of epoxy resin and Portland cement-based sealers with niobium and zirconium oxide radiopacifiers, Dent Mater. 30 (2014) 1005–1020. doi:10.1016/j.dental.2014.05.007.

[5] F. Monticelli, J. Sword, R.L. Martin, G.S. Schuster, R.N. Weller, M. Ferrari, D.H. Pashley, F.R. Tay, Sealing properties of two contemporary single-cone obturation systems, Int Endod J. 40 (2007) 374–385. doi:10.1111/j.1365-2591.2007.01231.x.

[6] M. Torabinejad, T.F. Watson, T.R. Pitt Ford, Sealing ability of a mineral trioxide aggregate when used as a root end filling material, J Endod. 19 (1993) 591–595. doi:10.1016/S0099-2399(06)80271-2.

[7] M.G. Gandolfi, S. Sauro, F. Mannocci, T.F. Watson, S. Zanna, M. Capoferri, C. Prati, R. Mongiorgi, New tetrasilicate cements as retrograde filling material: an in vitro study on fluid penetration, J Endod. 33 (2007) 742–745. doi:10.1016/j.joen.2007.02.008.

[8] M. Fridland, R. Rosado, MTA solubility: a long term study, J Endod. 31 (2005) 376–379.

[9] I. Islam, H.K. Chng, A.U.J. Yap, X-ray diffraction analysis of mineral trioxide aggregate and Portland cement, Int Endod J. 39 (2006) 220–225. doi:10.1111/j.1365-2591.2006.01077.x.

[10] M. Parirokh, M. Torabinejad, Mineral trioxide aggregate: a comprehensive literature review--Part III: Clinical applications, drawbacks, and mechanism of action, J Endod. 36 (2010) 400–413. doi:10.1016/j.joen.2009.09.009.

[11] M. a. A. De Bruyne, R.J.E. De Bruyne, L. Rosiers, R.J.G. De Moor, Longitudinal study on microleakage of three root-end filling materials by the fluid transport method and by capillary flow porometry, Int Endod J. 38 (2005) 129–136. doi:10.1111/j.1365-2591.2004.00919.x.

[12] S.S. Hakki, B.S. Bozkurt, B. Ozcopur, M.G. Gandolfi, C. Prati, S. Belli, The response of cementoblasts to calcium phosphate resin-based and calcium silicate-based commercial sealers, Int Endod J. 46 (2013) 242–252. doi:10.1111/j.1365-2591.2012.02122.x.

[13] P. Kitikuson, T. Srisuwan, Attachment Ability of Human Apical Papilla Cells to Root Dentin Surfaces Treated with Either 3Mix or Calcium Hydroxide, J Endod. 42 (2016) 89–94. doi:10.1016/j.joen.2015.08.021.

[14] J.S. Al-Sanabani, A.A. Madfa, F.A. Al-Sanabani, Application of calcium phosphate materials in dentistry, Int J Biomater. 2013 (2013) 876132. doi:10.1155/2013/876132.

[15] R. Osorio, E. Osorio, I. Cabello, M. Toledano, Zinc induces apatite and scholzite formation during dentin remineralization, Caries Res. 48 (2014) 276–290. doi:10.1159/000356873.

[16] F. Monticelli, R. Osorio, M. Toledano, M. Ferrari, D.H. Pashley, F.R. Tay, Sealing properties of one-step root-filling fibre post-obturators vs. two-step delayed fibre post-placement, J Dent. 38 (2010) 547–552. doi:10.1016/j.jdent.2010.03.014.
[17] P.J. Vizgirda, F.R. Liewehr, W.R. Patton, J.C. McPherson, T.B. Buxton, A comparison of laterally condensed gutta-percha, thermoplasticized gutta-percha, and mineral trioxide aggregate as root canal filling materials, J Endod. 30 (2004) 103–106. doi:10.1097/00004770-200402000-00010.
[18] M.G. Gandolfi, C. Prati, MTA and F-doped MTA cements used as sealers with warm gutta-percha. Long-term study of sealing ability, Int Endod J. 43 (2010) 889–901. doi:10.1111/j.1365-2591.2010.01763.x.
[19] H. Ryou, L.-N. Niu, L. Dai, C.R. Pucci, D.D. Arola, D.H. Pashley, F.R. Tay, Effect of biomimetic remineralization on the dynamic nanomechanical properties of dentin hybrid layers, J. Dent. Res. 90 (2011) 1122–1128. doi:10.1177/0022034511414059.
[20] W.C. Oliver, G.M. Pharr, An improved technique for determining hardness and elastic modulus using load and displacement sensing indentation experiments, Journal of Materials Research. 7 (1992) 1564–1583. doi:10.1557/JMR.1992.1564.
[21] M. Toledano, R. Osorio, E. Osorio, A.L. Medina-Castillo, M. Toledano-Osorio, F.S. Aguilera, Ions-modified nanoparticles affect functional remineralization and energy dissipation through the resin-dentin interface, J Mech Behav Biomed Mater. 68 (2017) 62–79. doi:10.1016/j.jmbbm.2017.01.026.
[22] M. Toledano-Osorio, E. Osorio, F.S. Aguilera, A. Luis Medina-Castillo, M. Toledano, R. Osorio, Improved reactive nanoparticles to treat dentin hypersensitivity, Acta Biomater. 72 (2018) 371–380. doi:10.1016/j.actbio.2018.03.033.
[23] M. Toledano, R. Osorio, E. Osorio, A.L. Medina-Castillo, M. Toledano-Osorio, F.S. Aguilera, Ions-modified nanoparticles affect functional remineralization and energy dissipation through the resin-dentin interface, J Mech Behav Biomed Mater. 68 (2017) 62–79. doi:10.1016/j.jmbbm.2017.01.026.
[24] J.H. Kinney, J.R. Gladden, G.W. Marshall, S.J. Marshall, J.H. So, J.D. Maynard, Resonant ultrasound spectroscopy measurements of the elastic constants of human dentin, J Biomech. 37 (2004) 437–441. doi:10.1016/j.jbiomech.2003.09.028.
[25] H. Xu, Q. Zheng, Y. Shao, F. Song, L. Zhang, Q. Wang, D. Huang, The effects of ageing on the biomechanical properties of root dentine and fracture, J Dent. 42 (2014) 305–311. doi:10.1016/j.jdent.2013.11.025.
[26] A. Hoppe, N.S. Güldal, A.R. Boccaccini, A review of the biological response to ionic dissolution products from bioactive glasses and glass-ceramics, Biomaterials. 32 (2011) 2757–2774. doi:10.1016/j.biomaterials.2011.01.004.
[27] M. Toledano, F.S. Aguilera, E. Osorio, I. Cabello, M. Toledano-Osorio, R. Osorio, Self-etching zinc-doped adhesives improve the potential of caries-affected dentin to be functionally remineralized, Biointerphases. 10 (2015) 031002. doi:10.1116/1.4926442.
[28] N.M.S. Leal, J.L. Silva, M.I.M. Benigno, E.A. Bemerguy, J.B.C. Meira, R.Y. Ballester, How mechanical stresses modulate enamel demineralization in non-carious cervical lesions?, J Mech Behav Biomed Mater. 66 (2017) 50–57. doi:10.1016/j.jmbbm.2016.11.003.
[29] H. Ryou, D.H. Pashley, F.R. Tay, D. Arola, A characterization of the mechanical behavior of resin-infiltrated dentin using nanoscopic Dynamic Mechanical Analysis, Dent Mater. 29 (2013) 719–728. doi:10.1016/j.dental.2013.03.022.

[30] V. Gopalakrishnan, C.F. Zukoski, Delayed flow in thermo-reversible colloidal gels, Journal of Rheology. 51 (2007) 623–644. doi:10.1122/1.2736413.
[31] R. Agrawal, A. Nieto, H. Chen, M. Mora, A. Agarwal, Nanoscale damping characteristics of boron nitride nanotubes and carbon nanotubes reinforced polymer composites, ACS Appl Mater Interfaces. 5 (2013) 12052–12057. doi:10.1021/am4038678.
[32] Y. Shinno, T. Ishimoto, M. Saito, R. Uemura, M. Arino, K. Marumo, T. Nakano, M. Hayashi, Comprehensive analyses of how tubule occlusion and advanced glycation end-products diminish strength of aged dentin, Sci Rep. 6 (2016) 19849. doi:10.1038/srep19849.
[33] J. Ivancik, D.D. Arola, The importance of microstructural variations on the fracture toughness of human dentin, Biomaterials. 34 (2013) 864–874. doi:10.1016/j.biomaterials.2012.10.032.
[34] R. Holland, Histochemical response of amputed pulps to calcium hydroxide, Rev Bras Pesq Med Biol. 4 (1971) 83–95.
[35] S. Sharma, V. Sharma, D. Passi, D. Srivastava, S. Grover, S.R. Dutta, Large Periapical or Cystic Lesions in Association with Roots Having Open Apices Managed Nonsurgically Using 1-step Apexification Based on Platelet-rich Fibrin Matrix and Biodentine Apical Barrier: A Case Series, J Endod. 44 (2018) 179–185. doi:10.1016/j.joen.2017.08.036.
[36] J.H. Kinney, S.J. Marshall, G.W. Marshall, The mechanical properties of human dentin: a critical review and re-evaluation of the dental literature, Crit. Rev. Oral Biol. Med. 14 (2003) 13–29.
[37] J.J. Kruzic, R.K. Nalla, J.H. Kinney, R.O. Ritchie, Crack blunting, crack bridging and resistance-curve fracture mechanics in dentin: effect of hydration, Biomaterials. 24 (2003) 5209–5221.
[38] M. Pérez Alvarez, J. Delgado García-Menocal, Almirall La Serna, H. Alfonso, J. Collins, M. Fernández Diaz, A. Márquez, J. Rodríguez Hernandez, C. Rodríguez, H. Somonte Dávila, R. Guerra Bretaña, A. Morejón, Use of cuban granulated B-Tricalcium Phosphate “Biograft-G” as maxilar bone graft, Journal of Oral Hygiene & Health. 1 (2013) 103–105.

Table 1. Materials and chemicals used in this study.

<table>
<tr><td colspan="4">Product details</td></tr>
<tr><td rowspan="3">Calcypatite</td><td rowspan="3">Calcium hydroxide $(CaOH)_2$
Paste</td><td colspan="2">Basic formulation per 100 gr</td></tr>
<tr><td>Content and quantity (g)</td><td>Percentage (%)</td></tr>
<tr><td>Calcium hydroxide 45.0 g
Carbowax 400 40.0 g
Titanium dioxide 7.0 g
Aerosil 1.0 g
Barium Sulphate 7.0 g</td><td>42.5</td></tr>
<tr><td rowspan="2">Hydroxyapatite particles: Synthetic dense ceramic granulate in hte form of shape irregular with grain size between 0.1 and 0.4 mm [38].</td><td>Component and percentage</td><td rowspan="2">57.5</td></tr>
<tr><td>Calcium 39.2 %
Phosphorus 18.3 %
Magnesium < 0.1 %
Sodium < 0.1 %
Silicon 0.001-0.03 %
Other minor components < 0.005 %

Molar relation Ca/P 1.66</td></tr>
<tr><td rowspan="4">Oxiapatite</td><td rowspan="3">Zinc oxide (ZnO)</td><td colspan="2">Basic formulation per 100 gr</td></tr>
<tr><td>Content and quantity (g)</td><td>Percentage (%)</td></tr>
<tr><td>Zinc oxide (grain size˜1µm) 39.61 g
Titanium dioxide 5.8 g
Carbowax 400 40.0 g
Aerosil 2.0 g
Barium sulphate 14.8 g</td><td>42.5</td></tr>
<tr><td rowspan="2">Hydroxyapatite particles: Synthetic dense ceramic granulate in hte form of shape irregular with grain size between 0.1 and 0.4 m [38].</td><td>Component and percentage</td><td rowspan="2">57.5</td></tr>
<tr><td>Calcium 39.2 %
Phosphorus 18.3 %
Magnesium < 0.1 %
Sodium < 0.1 %
Silicon 0.001-0.03 %
Other minor components < 0.005 %

Molar relation Ca/P 1.66</td></tr>
<tr><td colspan="2">AH Plus (Dentsply, DeTrey, Konstanz, Germany)</td><td colspan="2">Paste A: diepoxide, calcium tungstate, zirconium oxide, aerosil, pigment (Fe oxide)
Paste B: 1-adamantane amine, N,N’-dibenzyl-5-oxa-nonandiamine-1,9, TCD-Diamine, calcium tungstate, zirconium oxide, aerosil, silicone oil</td></tr>
<tr><td colspan="2">Guttacore (Dentsply Tulsa Dental Specialties, Tulsa, USA)</td><td colspan="2">Guttapercha; zinc oxide; bismuth oxide; 2,5-dimethyl-2,5di(tertbutylperoxy)hexane; titanium dioxide; para-amid fiber; silica,amorphous, precipitated; other components (<5%)</td></tr>
<tr><td colspan="4">NaOCl 5% (Panreac Química SA, Barcelona, Spain)</td></tr>
<tr><td colspan="4">EDTA 17% (Sigma Aldrich, St. Louis, MO, USA)</td></tr>
<tr><td rowspan="2">Simulated Body Fluid Solution (SBFS) pH=7.45</td><td>Sigma Aldrich, St. Louis, MO, USA</td><td colspan="2">NaCl 8.035 g
$NaHCO_3$ 0.355 g
$K_2HPO_4 \cdot 3H_2O$ 0.231 g, $MgCl_2 \cdot 6H_2O$ 0.311 g
1.0 M – HCl 39 ml
Tris 6.118 g</td></tr>
<tr><td>Panreac Química SA, Barcelona, Spain</td><td colspan="2">KCl 0.225 g
$CaCl_2$ 0.292 g
Na_2SO_4 0.072 g
1.0 M – HCl 0–5 ml</td></tr>
</table>

Abbreviations: SBFS: simulated body fluid solution; TCD: 3(4),8(9)-bis(aminomethyl)triciclo[5.2.1.02,6] Decane; NaCl: sodium chloride; $NaHCO_3$: sodium bicarbonate; KCl: potassium chloride; $K_2HPO_4 \cdot 3H_2O$: potassium phosphate dibasic trihydrate; $MgCl_2 \cdot 6H_2O$: magnesium chloride hexahydrate; HCl: hydrogen chloride; $CaCl_2$: Calcium chloride; Na_2SO_4: sodium sulfate; Tris: tris(hydroxylmethyl) aminomethane.

Table 2: Mean (SD) of Young's Modulus (GPa) measured at the experimental groups.

Young's Modulus (GPa)													
		Cervical				Middle				Apical			
		Inner zone		Outer zone		Inner zone		Outer zone		Inner zone		Outer zone	
		24 h	6 m	24 h	6 m	24 h	6 m	24 h	6 m	24 h	6 m	24 h	6 m
Materials	**Guttacore**	3.32 (0.27) a1*†	14.43 (0.60) A1†	6.52 (0.35) a2*†	12.71 (0.86) A2†	12.84 (1.45) a1‡	14.02 (2.48) A1†	4.73 (0.28) a2*‡	12.85 (2.80) A1†‡	13.99 (1.19) a1*‡	20.65 (1.25) A1‡	17.51 (0.70) a2§	18.06 (3.02) AB1‡
	AH Plus	16.64 (2.58) b1†	16.56 (2.99) A1†	18.26 (0.84) b1†	19.40 (1.11) B1†	16.72 (3.56) ab1†	20.46 (0.71) B1‡	14.11 (0.56) b1*‡	18.31 (1.00) B2†	20.82 (3.37) bc1*†	12.77 (0.59) B1§	18.97 (0.95) a1*†	7.36 (1.52) C2‡
	Calcypatite	24.74 (1.71) c1*†	14.26 (1.73) A1†	22.07 (0.81) c2*†	17.67 (0.47) C2†	17.98 (1.41) b1*‡	9.04 (0.25) C1‡	14.02 (0.40) b2‡	13.98 (3.06) A2‡	15.09 (2.72) ab1‡	23.77 (6.67) AC1§	13.49 (0.65) b1*‡	16.99 (1.42) A1†‡
	Oxipatite	14.84 (2.87) b1*†	21.69 (1.62) B1†	9.53 (0.71) d2*†	27.75 (1.25) D2†	32.11 (13.52) b1*‡	17.05 (1.22) A1‡	23.76 (2.33) c1*‡	16.77 (2.70) AB1‡	21.19 (2.56) c1*‡	25.99 (1.11) C1§	18.93 (1.27) a1§	23.33 (3.88) B1‡

Identical lower case indicates no significant differences among different materials at the same dentin third (cervical/medial/apical) and zones (inner/outer) after 24 hours. Identical capital letter indicates no significant differences between different materials at the same dentin third (cervical/medial/apical) and zones (inner/outer) after 6 months. Identical number indicates no significant differences between different zones (inner/outer) with the same materials at the same storage time. Asterisks indicate significant differences between different storage periods (24 h/6 m) with the same material at the same zone (inner/outer). Identical symbol indicates no significant differences between different dentin thirds (cervical/medial/apical) at the same zone (inner/outer) and period (24 h/6 m) with the same material, after Student-Newman-Keuls or Student t tests respectively ($p<0.05$).

Figure 1. (**a**) Schematic illustration indicating how dentin permeability was measured. Specimens were connected to a hydraulic pressure device under a constant hydraulic pressure. The measurements of the changes in fluid volume were attained via a digital sensor. (**b**) Schematic representation of the **s**pecimen preparation for interfacial evaluation Tooth coronal section was discarded. Three disks of cervical, medial and apical dentin were obtained. Inner and outer dentin zones were assessed.

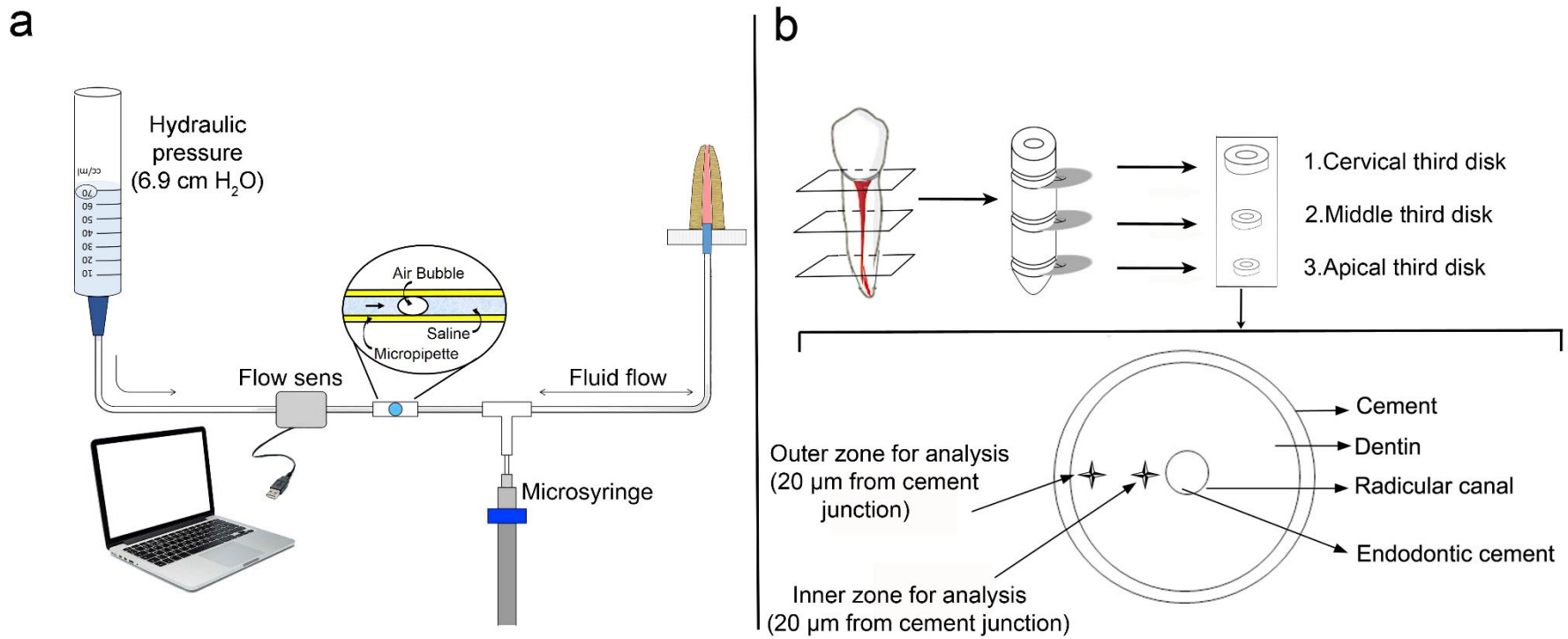

Figure 2. Attained microleakage values (mean and SD) for each canal sealer. Letters indicate differences between canal sealers at each time point and numbers identify differences between time points within the same canal sealer ($p < 0.05$).

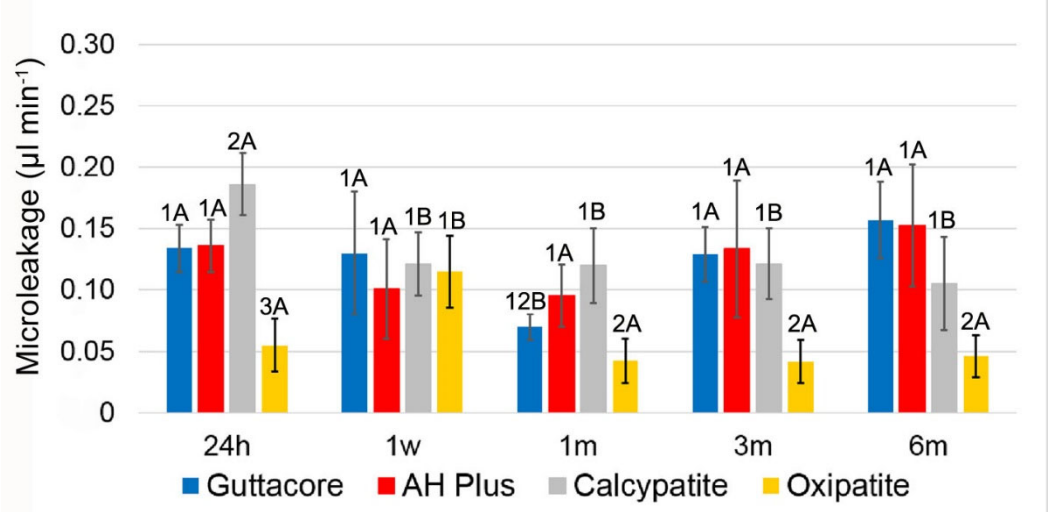

Figure 3. (a) 10 x 10 µm topographic mapping obtained by AFM at the inner zone of the apical dentin treated with oxipatite, after 6 m of storage. Minerals allowed a restricted display of the tubule entrances (arrows) or a complete sealing of the lumen of tubules which figured completely occluded (arrowheads). (**b**) 10 x 10 µm topographic mapping of inner zone of cervical dentin infiltrated with calcypatite after 6 m of storage, obtained by AFM. Peritubular dentin appeared strongly remineralized (double arrows). (**c**) 10 x 10 µm topographic mapping obtained by AFM at the inner zone of the cervical dentin treated with AH Plus, after 6 m of storage. Underlying collagen fibers, which show the staggered pattern of collagen fibrils, produced great prominence resulting clearly visible (arrowheads). (**d**) 10 x 10 µm topographic mapping obtained by AFM at the inner zone of the cervical dentin treated with guttacore, after 6 m of storage. Dentinal tubules appeared permeable (arrows). Peritubular dentine is present (double arrows) or absent (arrowheads). A large platform of intertubular dentin (asterisks) protruded over almost absent peritubular dentin

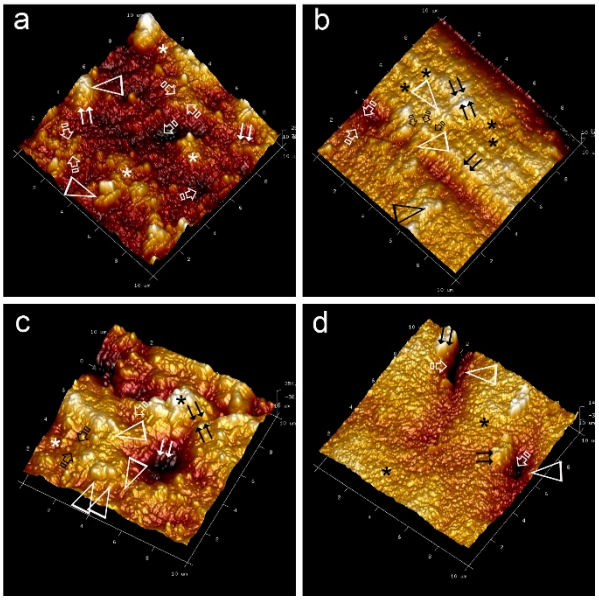

Figure 4.

Representative FESEM topographic images at root inner dentin surfaces treated with oxipatite were observed at both cervical (a) and apical thirds (b, c), at 6 m time point. Mineral deposition is completely filling the lumen of dentinal tubules (arrows) at dentin (a·I, b·II). Tubules resulted almost totally mineralized, and hermetically sealed, and the canal sealer (CS) did not allow any display of the entrance of tubules. Some tubular areas remained unfilled (arrowheads), but peritubular dentin appeared strongly mineralized (double arrows) (b·I, b·II). Zinc-based salts [phosphorous (P), calcium (Ca), and zinc (Zn)] aggregates were detected in the elemental analysis [EDX spectrum 1 and 2 at a·II, a·III, a·IV, b·II and b·III)]. Representative FESEM topographic images at the inner zone of the cervical (d), medial (e) and apical (f) dentin treated with calcypatite, after 6 m of storage. Dentinal tubules were partially mineral filled, allowing multiple empty spaces (arrows). Some tubules appeared mineral free but with a robust peritubular dentin wall (double arrows) (e·I). Spectrum from energy dispersive analysis, attained at spectrum 1 and 2 (f·II) is showing elemental composition; phosphorous (P) and calcium are encountered (Ca) (f·III, f·IV). AH Plus applied at the inner zone of the apical third, after 6 m of storage, was shown (g).The resin-dentin interface shows a lack of adaptation between both substrates (arrowheads). Low magnification of representative view of calcypatite (I) and oxipatite (II) placed in the apical third of root dentin, at 6 m time point (h).

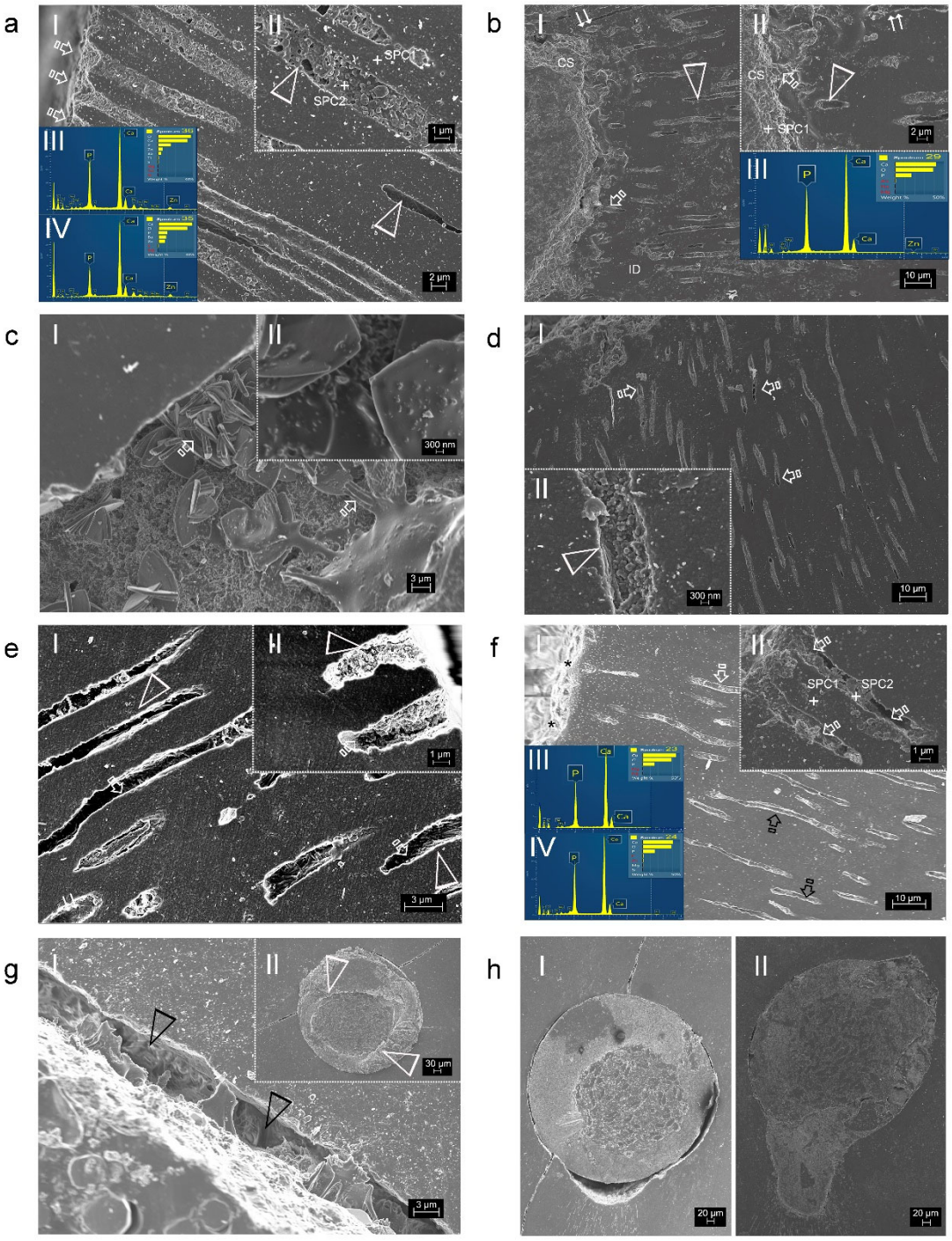
a
I
II
SPC1
SPC2
III
IV
1 µm
2 µm
b
I
II
CS
CS
SPC1
ID
III
2 µm
10 µm
c
I
II
300 nm
3 µm
d
I
II
300 nm
10 µm
e
I
II
1 µm
3 µm
f
I
II
SPC1
SPC2
III
IV
1 µm
10 µm
g
I
II
30 µm
3 µm
h
I
II
20 µm
20 µm

Acknowledgements

This work was supported by the Ministry of Economy and Competitiveness (MINECO) and European Regional Development Fund (FEDER). Project MAT2017-85999-P MINECO/AEI/FEDER/UE.